Par-Cteno-Genesis or Cteno Par-Genesis

Authors:

Miguel Salinas-Saavedra[1]* and Mark Q Martindale[1]

Affiliation:

[1] The Whitney Laboratory for Marine Bioscience, and the Department of Biology, University of Florida, 9505 N, Ocean Shore Blvd, St. Augustine, FL 32080-8610, USA

*Corresponding author

Email: mssaavedra@whitney.ufl.edu; mssaavedra@gmail.com (MS-S)

ABSTRACT

In bilaterians and cnidarians, embryonic and epithelial cell-polarity are regulated by the interactions between Par proteins, Wnt/PCP signaling pathway, and cell-cell adhesion. Par proteins are highly conserved across Metazoa, including ctenophores. But strikingly, ctenophore genomes lack components of the Wnt/PCP pathway and cell-cell adhesion complexes; raising the question if ctenophore cells are polarized by mechanisms involving Par proteins. Here, by using immunohistochemistry and live-cell imaging overexpression of specific mRNAs, we describe for the first time the subcellular localization of selected Par proteins in blastomeres and epithelial cells during the embryogenesis of the ctenophore *Mnemiopsis leidyi*. We show that these proteins distribute differently compared to what has been described for other animals. This differential localization might be related with the emergence of different junctional complexes during Metazoa evolution. Data obtained here challenge the ancestry of the apicobasal cell polarity and raise questions about the homology of epithelial tissue across the Metazoa.

INTRODUCTION

The emergence of epithelial tissues was arguably one of the most critical events in animal evolution. In bilaterians and cnidarians, a true epithelium is defined as a group of polarized cells joined by belt-like cell-cell junctions and supported by a basement membrane, that can regulate passage of molecules paracellularly. Epithelial cells are polarized along the apical-basal axis and form a planar sheet of cells that can undergo subsequent morphogenesis[1–5]. While the asymmetric cortical distribution of the Wnt Planar Cell Polarity (PCP) pathway components polarizes the cells along the tissue plane, the asymmetric cortical distribution of Par system components polarizes the cells along the apical-basal axis[2,3,5–19]. These mechanisms that organize cell-polarity are highly conserved in all animals that have been studied and most likely they must have been present in the most recent common ancestor (MRCA) of Cnidaria and Bilateria[3,5,16,18,20–23]. However, little is known outside of those two clades (Figure 1A).

Interestingly, ctenophores or comb jellies, currently hypothesized to be the sister taxa to all metazoans[24–28], do not have the genes that encode the components of the Wnt/PCP pathway in their genomes[26]. Thus, the study of the subcellular organization of the Par system components in ctenophores and their potential role in apical-basal polarity is important to understand the evolution of tissue organization in Metazoa.

The asymmetric localization of the Crumbs (Crb) complex, (e.g. Crb/Pals1/Patj), the Par/aPKC complex (e.g. Par-3/aPKC/Par-6), and the Scribble complex (e.g. Scribble/Lgl/Dlg) in the cortex of bilaterian and cnidarian cells maintains epithelial integrity by stabilizing cell-cell junctions[4,5,20,22,23]. When the Par/aPKC complex is activated by Cdc42, they bind to the apical cortex via the Crb complex[4,29–31], and recruits and stabilizes E-cadherin[4,22,32–34]. E-cadherin, in turn, sequesters ß-catenin from the cytoplasm that binds to alpha-catenin and links this protein complex to the actin cytoskeleton, thus stabilizing Adherens Junctions (AJs)[1,23,33,35–39]. The maturation of AJs it is essential for the maintenance of the Par/aPKC complex localization at the apical cortex that

displaces members of the Scribble complex and Par-1 to basolateral localizations associated with Septate Junctions (SJs)[23,40–48]. The regulation of AJs is, therefore, critical for the maintenance of epithelial polarity and its function regulating epithelial physiology[21,22,34,49–51].

This mechanism is deployed in metazoan cells to establish embryonic and epithelial cell polarity during early development and is critical for axial organization[5,15,17,21,22,34,52–67]. In most bilaterian animals cell symmetry breaking is mediated by the Par system set up maternally during the first cleavage stages[5,58,68,69]. While the Par system establishes and maintains the asymmetric localization of junctional complexes in epithelial cells, during development the asymmetric localization of Par proteins ensures the proper partitioning of maternal determinants into distinct daughter cells during the stereotyped cleavage program in bilaterians[3,15,53,58]. This is not the case in cnidarians (e.g. corals, sea anemones and “jellyfish) that do not possess a stereotyped cell division pattern[5,70,71]. Intriguingly, ctenophores (comb jellies like *Mnemiopsis leidyi*), that are thought to be an even more ancient group of animals[24,26,28], develop under a highly determined and stereotyped developmental program[72–75] (Figure 1B). Therefore, the description of Par protein localization would give insights on how cell polarity is deployed during these early stages.

Components of the Par system are highly conserved across Metazoa, including ctenophores[20,23]. But strikingly, ctenophore genomes also do not have many of the crucial regulators present in bilaterian and cnidarian genomes[23,46]. For example, none of the components of the Crb complex, a Scribble homolog, SJs, are present, and the cytoplasmic domain of cadherin lacks the crucial biding sites to catenins that interact with the actin cytoskeleton[23]. These data raise the question of whether or not ctenophore cells are polarized by mechanisms involving the apicobasal cell polarity mediated by Par proteins and question the homology of epithelial tissue across the Metazoa. Here, by using antibodies raised to specific ctenophore proteins and confirmed by live-cell imaging of injected fluorescently labeled mRNAs, we describe for the first time the subcellular localization of selected components of the Par system during the development of the

ctenophore *Mnemiopsis leidyi*. Data obtained here challenge the ancestry of the apicobasal cell polarity module, suggest that AJs and SJs are not required to polarize animal cells, and raise questions about the ancestral structure and function of epithelial tissue in the Metazoa.

RESULTS

Antibody Specificity

Components Genome searches of *M. leidyi* showed there were only a single copy for both Par-6 (*Ml*Par-6) and Par-1 (*Ml*Par-1) genes. Rabbit polyclonal affinity-purified antibodies (Bethyl labs, Inc) designed against *M. leidyi Ml*Par-6 and *Ml*Par-1 were used to determine their spatial and temporal expression at different developmental stages. Each antibody was characterized by Western blotting to establish its specificity (Figure 2A). Western blots of *M. leidyi* adult extracts showed that the antibodies recognized different bands for *Ml*Par-6 (predicted size 33.3 KD; Figure 2A) and *Ml*Par-1 (predicted size 84.7 KD; Figure 2A) indicating that each antibody recognizes different genes. Pre-adsorption of the *Ml*Par-6 and *Ml*Par-1 antibody with a tenfold molar excess of the respective antigenic peptide (used to generate and affinity purify the antibodies) resulted in the elimination of the appropriate-sized single band for *Ml*Par-6 and *Ml*Par-1 (Figure 2A). In addition, whole-mount immunohistochemistry pre-adsorption experiments were performed to test the specificity of the *Ml*Par-6 and *Ml*Par-1 antibodies. The staining pattern was strongly mitigated in early embryos when pre-incubated antibodies were used (Figure 2B). Thus, both antibodies are specific to their intended targets and provide robust reagents to determine the subcellular localization of these proteins during ctenophore embryogenesis. structure and function of epithelial tissue in the Metazoa.

*Ml*Par-6 Gets Localized to the Apical Cortex of Cells During Early *M. leidyi* Development

Using our specific *Ml*Par-6 antibody we characterized the subcellular localization of the *Ml*Par-6 protein during early *M. leidyi* development. In all of the over 100 specimens examined,

*Ml*Par-6 expression polarizes to the animal cortex (determined by the position of the egg pronucleus; Figure 3A) of the single cell zygote and to the apical cell cortex (cell-contact-free regions facing the external media) during every cleavage stage (Figure 3). At the cortex, *Ml*Par-6 localizes perpendicular to the cleavage furrow in cell-contact-free regions (Figure 3B). In addition, as cleavage ensues, *Ml*Par-6 becomes localized to the position of cell-cell contacts between blastomeres until gastrulation (Figure 3A). When the embryo is gastrulating (3-7 hpf), *Ml*Par-6 is not localized in cells undergoing cellular movements including the animal (4 hpf; Figure 4A) and vegetal ectoderm (5 hpf; Figure 4A) that are undergoing epibolic movements, syncytial endoderm, and mesenchymal 'mesoderm.' However, this protein remains apically polarized in 'static' ectodermal cells remaining at the animal pole (blastopore) and vegetal pole. By the end of gastrulation (8-9 hpf; Figure 5A), *Ml*Par-6 becomes localized in the apical cortex of the ectodermal epidermal cells and is also asymmetrically localized in the future ectodermal pharyngeal cells that start folding inside the blastopore (Figure 5A). Interestingly, no clear cortical localization was observable in later stages and the antibody signal is weak after 10 hpf. Contrary to what was expected, in these later stages, *Ml*Par-6 is localized to the cytoplasm and does not localize in the cortex of epidermal cells and few epithelial and mesenchymal cells showed nuclear localization (Figure 5A), suggesting the protein does not play a role in cell adhesion or cell polarity during those stages.

Similar results were obtained when the mRNA encoding for *Ml*Par-6 fused to mVenus (*Ml*Par-6-mVenus) was overexpressed and the in vivo localization of the protein was recorded in *M. leidyi* embryos (Figure 5B). In these experiments, the translated *Ml*Par-6-mVenus was observed after 4 hours post injection into the uncleaved egg. *M. leidyi* develops rapidly with cell cycle times of 15 minutes between cleavages, and therefore, it was impossible at this time to observe the in vivo localization of this protein in early blastomeres. During gastrulation, *Ml*Par-6-mVenus localizes to the apical cell cortex and displays enrichment at the level of cell-cell contacts (Figure 5B). However, as we observed by antibody staining, this cortical localization is no longer observable during the cell

movements associated with gastrulation and *Ml*Par-6-mVenus remains cytosolic (Figure 5B). After 8 hpf, *Ml*Par-6-mVenus localizes to the apical cortex of ectodermal epidermal and pharyngeal cells but is not observable in any other internal tissue (Figure 5B). After 10 hpf, *Ml*Par-6-mVenus remains in the cytosol and no cortical localization was detectable (Figure 5B), confirming the antibody observations presented above.

*Ml*Par-1 Remains Cytoplasmic During Early *M. leidyi* Development

In bilaterians and cnidarians, the apical localization of *Ml*Par-6 induces the phosphorylation of *Ml*Par-1 displacing this protein to basolateral cortical regions[4,5,21,22]. Using our specific *Ml*Par-1 antibody we characterized the subcellular localization of the *Ml*Par-1 protein during the early *M. leidyi* development (Figure 6 and Figure 7). Even though *Ml*Par-1 appears to be localized in the cortex at the cell-contact regions of early blastomeres (Figure 6B) and gastrula stages (Figure 7), this antibody signal was not clear enough to be discriminated from the cytosolic distribution. Nevertheless, and strikingly, *Ml*Par-1 remains as punctate aggregations distributed uniformly in the cytosol, and in some cases, co-distributes with chromosomes during mitosis (Figure 6 and Figure 7), but no asymmetric localization of *Ml*Par-1 was observed in the cell cortex of *M. leidyi* embryos at any of the stages described above for *Ml*Par-6.

These Similar results were observed in vivo when the mRNA encoding for *Ml*Par-1 fused to mCherry (*Ml*Par-1-mCherry) was overexpressed into *M. leidyi* embryos by microinjection (Figure 8A). Similar to *Ml*Par-6-mVenus mRNA overexpression, the *Ml*Par-1-mCherry translated protein was observed after 4 hours post injection into the uncleaved egg and its early localization in blastomeres was too faint to detect by this method. Our in vivo observations confirm the localization pattern described above using *Ml*Par-1 antibody at gastrula stages. *Ml*Par-1-mCherry localizes uniformly and form aggregates in the cytosol during gastrulation (4-5 hpf; Figure 8A). This localization pattern remains throughout all recorded stages until cydippid larva where *Ml*Par-1-

mCherry remains cytosolic in all cells but is highly concentrated in the tentacle apparatus and underneath the endodermal canals (24 hpf; Figure 8A).

Interestingly, the punctuate aggregates of *Ml*Par-1-mCherry are highly dynamics and move along the entire cytoplasm suggesting a potential association with cytoskeletal components (Movie 1). Unfortunately, we were not able to clone and express neither *Ml*Dlg nor *Ml*Lgl to observe if they resemble similar localization patterns in vivo.

*Ml*Par-6 and *Ml*Par-1 Structures are Conserved

In bilaterians To discount the possibility that the observations recorded in vivo for both *Ml*Par-6-mVenus and *Ml*Par-1-mCherry proteins are caused by a low-quality mRNA or lack of structural conservation, we overexpressed each ctenophore mRNA into embryos of the cnidarian *Nematostella vectensis* and followed their localization by in vivo live-cell imaging (Figure 8B). In these experiments, both *Ml*Par-6-mVenus and *Ml*Par-1-mCherry translated proteins display the same pattern than the previously described endogenous *N. vectensis* proteins [5]. In *N. vectensis* embryos, *Ml*Par-6-mVenus and *Ml*Par-1-mCherry symmetrically localize during early cleavage stages and both protein asymmetric localization was observable only after blastula formation (Figure 8B). These data not only suggest that the ctenophore *Ml*Par-6 and *Ml*Par-1 protein structure and function are conserved but also indicate that their subcellular localization in *M. leidyi* embryos is regulated by an interaction with other signaling pathways that is different than *N. vectensis* embryos.

*Ml*Cdc42 and *Ml*aPKC

To expand our observations on the localization of Par system components, we separately overexpressed the mRNA encoding for *Ml*Cdc42 fused to mCherry (*Ml*Cdc42-mCherry) and *Ml*aPKC fused to mVenus (*Ml*aPKC-mVenus). Both *Ml*Cdc42-mCherry (Figure 8C) and *Ml*aPKC-mVenus (Figure 8D) translated protein were observable and recorded after 3 to 4 hours post

injection into the uncleaved egg. Surprisingly, *Ml*Cdc42-mCherry only localizes in the cytosol and form punctate aggregates without any clear cortical localization through all stages recorded (Figure 8C). On the other hand, *Ml*aPKC-mVenus displayed an apparent apical localization but the signal of the translated protein was not strong enough to discriminate this localization from the cytosolic protein (Figure 8D). Even though these data give some insights on the localization of both *Ml*Cdc42-mCherry and *Ml*aPKC-mVenus proteins, the development of specific antibodies is required to determine the localization of maternally loaded proteins and discard technical artifacts. Unfortunately, we were not able at this time to co-inject these proteins together in order to see their in vivo interactions during embryonic development. Further technical improvements beyond the purposes of this work are necessary.

DISCUSSION

Cell Polarity is Established but not Maintained by PAR Proteins During *M. leidyi* Embryogenesis

The early polarization of the Par/aPKC complex seems to be a conserved characteristic of stereotyped cleavage patterns in bilaterians where the Par system has been studied[4,5,14,15,53,56–59,63,66,68,69,76–80]. In these species, the asymmetric localization of Par-6 and Par-1 has been used as an indicator of maternal partitioning of determinants[58,61,63,69,81,82]. Ctenophores embryos divide by a highly stereotyped and polarized developmental pattern where blastomeres are already determined[73–75,83–85]. The asymmetrical localization of the zygotic nucleus and spindle apparatus along with *Ml*Par-6 to the animal pole in the uncleaved egg and the apical cortex of blastomeres (Figure 3) is an indicator that the cells of *M. leidyi* are highly polarized by maternally loaded proteins as in other bilaterian animals. Even though this cortical polarization of *Ml*Par-6 is maintained during gastrulation in the ectoderm (Figure 4), epithelial cells of later stages do not display an asymmetric localization of *Ml*Par-6 (Figure 5). Thus, the cell polarity established during earlier stages (characterized by the apical localization of *Ml*Par-6) is not maintained by PAR proteins when

definitive ctenophore epithelial tissues form. Conversely, the subcellular localization of *Ml*Par-1 does not display a clear polarization during any of the observed developmental stages (Figures 6 to 8). Instead, punctate aggregates distribute symmetrically and actively migrate throughout the cytosol. This is particularly surprising compared to cnidarian development where there is no localization of any of the Par components early, but these become highly polarized when epithelial tissues form[5,21].

Even though the mechanism that induce and establish the asymmetrical localization of Par proteins in the cell cortex during early animal development remains unknown, the maintenance of the apicobasal cell polarity in mature epithelial tissue is carried out by a conserved and well-studied mechanism. In the cnidarian *N. vectensis* and bilaterian embryos, mature and stable AJs and SJs stabilize the cytoskeleton of the cell cortex and allow the proper polarization of the cell along the apical-basal axis[4,5,86,17,20,22,23,46,61,69,81]. The proper positioning of AJs and SJs complexes allows them to physically separate the apical domain from the basolateral domain of the cell cortex, respectively. The apical cortex is defined by the stable localization of the Crb complex and the interaction between the cytoskeleton and the Cadherin-Catenin complex (CCC)[4,20,23,87,88]. The stabilization of the lateral cortex cytoskeleton, on the other hand, depends on the stable interaction between SJs and the Scribble complex[20,23,42,44–47,89]. Mutations in any of the components that conform these complexes in bilaterian embryos results in a mislocalization of polarity proteins and the junctional complexes disassembling[4,22,43,44,46,47,49–51].

Recent studies have shown that ctenophore species do not have the molecular components to form SJs and lack a Scribble homolog[23,46]. This suggests that none of the lateral polarity proteins (Dlg, Lgl, and Par-1) can localize to the lateral cortex of the ctenophore cells and explains the cytosolic localization of *Ml*Par-1 during the observed stages. The primary structure of *Ml*Par-1 protein (a Serine/threonine-protein kinase) is highly conserved and contains all the domains (with the same amino acid length) required for its proper functioning in other metazoans[20,23], and

localizes appropriately when expressed in cnidarian embryos (Figure 8B). Hence, the lack of SJs and Scribble proteins in ctenophore may affect the lateral localization of *Ml*Par-1 (polarity activity[40,43,47,90,91]) but not its other kinase functions in the cytoplasm (e.g., microtubule regulation[92–95]).

It has been also shown that ctenophores do not have mature AJs as we know them in other metazoans[1,23]. The cadherin of ctenophores does not have the cytoplasmic domains required to bind any of the catenins of the CCC (e.g. p120, alpha- and ß-catenin)[23]. This implies that neither the actin nor microtubule cytoskeleton can be linked to ctenophore cadherin through the CCC, as seen in other metazoans. In addition, ctenophores do not have homologous for any of the Crb complex components[23], required for the proper stabilization of the CCC and Par/aPKC complex in other studied taxa[4,31,35,62,96,97]. The lack of *Ml*Par-6 (Figure 5) and *Ml*Cdc42 (Figure 8C) polarization during later stages is totally congruent with these observations, indicating that PAR proteins in ctenophores do not have the interactions necessary and are not able to stabilize apico-basal cell polarity in their cells.

Similar to *Ml*Par-1, the components of the *Ml*Par/aPKC complex (*Ml*Par-3/*Ml*aPKC/*Ml*Par-6 and *Ml*Cdc42) are highly conserved and contain all the domains present in other metazoans[20,23]. Therefore, they are not only able to phosphorylate and displace *Ml*Par-1 and *Ml*Lgl to the cytoplasm but also are able to interact with Crb and localize to the apical cortex (Figure 8B). However, there are no Crb complexes nor AJs to interact with the Par/aPKC complex in ctenophore cells. The conservation of *Ml*Par-6 protein structure and apical localization during early cleavage stages also means that *Ml*Par-6 might be able to interact with cadherin, but that the Crb complex is not required for its polarization.

Evolution of Cell Polarity in Metazoa

In bilaterians the asymmetric localization of the components of the Par system establishes apicobasal cell polarity at the very early stages of embryonic development[4,5,17,69], controlling their characteristic stereotyped cleavage patterns. However, in the cnidarian *N. vectensis*, embryonic polarity is controlled by the Wnt signaling system[16,71,98–100]. The asymmetric localization of Par system components is established after cell-cell junctions are already from in the blastula epithelium and has no role on the early cleavage patterns[5]. In spite of these differences, in both bilaterian and cnidarian species, Par-mediated apicobasal cell polarity is responsible for the maturation and maintenance of cell-cell adhesion in epithelial tissue[4,22]. This suggests that the polarizing activity of the Par system was already present in epithelial cells of the MRCA between Bilateria and Cnidaria, whereas the role of the Par system directing early cleavage patterns could have been heterochronically co-opted during stem-Bilateria evolution.

The subcellular localization of some components of the Par system during the *M. leidyi* developmental stages studied here (Figure 3 to 8) challenges this hypothesis. The localization of *Ml*Par6 in cells of the ctenophore *M. leidyi* suggests that Par proteins are animally, but not vegetal, polarized in their egg prior to the first cleavage. Using *Ml*Par-6 as an indicator, we can conclude that an apical cell polarization is present during early cleavage stages and differentially regulated during gastrulation, but it is absent from epithelial cells of later juvenile stages. Unless the embryonic cell polarity in ctenophores is mediated by a completely different mechanism than bilaterians (that is also highly likely), our data would imply that cnidarians, such as *N. vectensis*, lost the mechanism by which Par proteins asymmetrically localize during early cleavage stages and gain a mechanism to maintain apicobasal cell polarity in epithelial tissues.

Intriguingly, ctenophore genomes do not have the full set of cell-cell adhesion[23,26,46] and Wnt signaling pathway components[26,27,101] that control the activity of Par proteins in bilaterian and cnidarian embryos. For example, in bilaterians the Wnt/PCP signaling pathway antagonizes the

action of the Par/aPKC complex[7,10,15,47,102,103], so this may explain the lack of polarization. In addition, the establishment of mature AJs and SJs is essential for the maintenance of cell polarity in cnidarian and bilaterian cells, so the absence of these pathways in ctenophores implies that a new set of interactions emerged at least in the Cnidaria+Bilateria ancestor, and that, could have regulated the way by which the Par system polarizes embryonic and epithelial cells (Figure 9). Furthermore, it would be also interesting to asses if the asymmetric localization of *Ml*Par-6 in *M. leidyi*, like in bilaterians, has roles related with the orientation of cell divisions and the establishment of cell-cell adhesion. Unfortunately, due to technical difficulties we are unable yet to test the function of maternally loaded *Ml*Par proteins during the early development of *M. leidyi*. To solve this question, further research in a larger sample of non-bilaterians animals is required.

In conclusion, we have shown that regardless of the high structural conservation of Par proteins across Metazoa, including ctenophores, ctenophore cells do not have other essential components to deploy the asymmetrical polarizing function of the Par system as in other studied metazoans. These results reinforce the idea that signaling pathways act as modules that interact with each other to organize the cells[104–106]. Recent genomic studies have shown that, during animal evolution, different signaling pathways components have emerged at different nodes of the metazoan tree[23,26,28]. Interestingly, ctenophore genomes suggest that new signaling pathways do not only emerge as individual components but also as a full set of protein complexes that bring a new set of interactions that remodel the cell structure and behavior. In agreement with genomic studies, our results challenge the conception of a deep homology of the epithelial structure in Metazoa and suggest that, regardless the genetic background, similar morphologies (e.g., epidermis and mesoderm) could be developed by similar cellular behaviors.

METHODS

Culture and Spawning of *M. leidyi*

Spawning, gamete preparation, fertilization and embryo culturing of *M. leidyi* embryos was performed as previously described[107]. Adult *M. leidyi* were maintained at the Whitney Laboratory for Marine Bioscience of the University of Florida (USA). Spawning was induced by incubating the adults under a three to four-hour dark cycle at room temperature. The embryos were kept in glass dishes (to prevent sticking) in filtered 1x seawater at room temperature until the desired stage.

Western Blot

Western blots were carried out as described[5,22] using adult tissue lysates dissected by hand in order to discard larger amount of mesoglea. Antibody concentrations for Western blot were 1:1,000 for all antibodies tested.

Immunohistochemistry

All immunohistochemistry experiments were carried out using the previous protocol for *M. leidyi*[107]. Embryos were fixed on a rocking platform at room temperature. Embryos of different stages were fixed for 2 hours in fresh Fixative (100mM HEPES pH 6.9; 0.05M EGTA; 5mM MgSO4; 200mM NaCl; 1x PBS; 3.7% Formaldehyde; 0.2% Glutaraldehyde; 0.2% Triton X-100; and 1X fresh sea water). Fixed embryos were rinsed at least five times in PBT (PBS buffer plus 0.1% BSA and 0.2% Triton X-100) for a total period of 3 hours. PBT was replaced with 5% normal goat serum (NGS; diluted in PBT) and fixed embryos were blocked for 1 to 2 hours at room temperature with gentle rocking. Primary antibodies were diluted in 5% NGS to desired concentration. Blocking solution was removed and replaced with primary antibodies diluted in NGS. All antibodies incubations were conducted over night on a rocker at 4°C. After incubation of the primary antibodies, samples were washed at least five times with PBT for a total period of 3 hours. Secondary antibodies were then applied (1:250 in 5% NGS) and samples were left on a rocker

overnight at 4°C. Samples were then washed with PBT and left on a rocker at room temperature for an hour. Samples were then washed once with PBT and incubated with DAPI (0.1µg/µl in PBT; Invitrogen, Inc. Cat. # D1306) for 1 hour to allow nuclear visualization. Stained samples were rinsed again in PBS two times and dehydrated quickly into isopropanol using the gradient 50%, 75%, 90%, and 100%, and then mounted in Murray's mounting media (MMM; 1:2 benzyl benzoate:benzyl alcohol) for visualization. Note that MMM attenuates the DAPI signal from samples. We scored more than 1,000 embryos per each antibody staining and confocal imaged more than 50 embryos at each stage obtaining similar staining patterns for each case.

The primary antibodies and concentrations used were: mouse anti-alpha tubulin (1:500; Sigma-Aldrich, Inc. Cat.# T9026. RRID:AB_477593). Secondary antibodies are listed in Key resources table.

Rabbit anti-*Ml*Par-6, and rabbit anti-*Ml*Par-1 antibodies are custom made high affinity-purified peptide antibodies that were raised by Bethyl labs Inc.). Affinity-purified *M. leidyi* anti-Par-6 (anti-*Ml*Par-6) and anti-Par-1 (anti-*Ml*Par-1) peptide antibodies were raised against a selected amino acid region of the *Ml*Par-6 protein (MTYPDDSNGGSGR; Bethyl Inc., Montgomery, TX, USA) and *Ml*Par-1 protein (KDIAVNIANELRL; Bethyl Inc., Montgomery, TX, USA), respectively. Blast searches against the *M. leidyi* genome sequences showed that the amino acid sequences were not present in any predicted *M. leidyi* proteins other than the expected protein. Both antibodies are specific to *M. leidyi* proteins (Figure 2) and were diluted 1:100.

mRNA Microinjections

The coding region for each gene of interest was PCR-amplified and cloned into pSPE3-mVenus or pSPE3-mCherry using the Gateway system[108]. Eggs were injected directly after fertilization as previously described for *N. vectensis* studies[5,109,110] with the mRNA encoding one or more proteins fused in frame with reporter fluorescent protein (N-terminal tag) using final concentrations of 300 ng/µl for each gene. Fluorescent dextran was also co-injected to visualize the

embryos. Live embryos were kept at room temperature and visualized after the mRNA of the FP was translated into protein (4-5 hours). Live embryos were mounted in 1x sea water for visualization. Images were documented at different stages. We injected and recorded 20 embryos for each injected protein and confocal imaged each specimen at different stages for detailed analysis of phenotypes in vivo. We repeated each experiment at least five times obtaining similar results for each case. The fluorescent dextran and primers for the cloned genes are listed in Key resources table.

Imaging of *M. leidyi* Embryos

Images of live and fixed embryos were taken using a confocal Zeiss LSM 710 microscope using a Zeiss C-Apochromat 40x water immersion objective (N.A. 1.20). Pinhole settings varied between 1.2-1.4 A.U. according to the experiment. The same settings were used for each individual experiment to compare control and experimental conditions. Z-stack images were processed using Imaris 7.6.4 (Bitplane Inc.) software for three-dimensional reconstructions and FIJI for single slice and movies. Final figures were assembled using Adobe Illustrator and Adobe Photoshop.

ACKNOWLEDGMENTS

We thank C.E. Schnitzler and J. Ryan for technical assistance with the ctenophore genome. This research was supported by the NSF IOS-1755364 and NASA 16-EXO16_2-0041 from MQM.

AUTHOR CONTRIBUTIONS

MS-S., and MQM. designed research and analyzed data. MS-S. performed research with help of MQM. MS-S., and MQM. wrote the manuscript. All authors read and approved the final manuscript.

DECLARATION OF INTERESTS

The authors declare no competing interests.

REFERENCES

1. Magie, C. R. & Martindale, M. Q. Cell-cell adhesion in the cnidaria: insights into the evolution of tissue morphogenesis. *Biol. Bull.* **214,** 218–232 (2008).
2. Johnston, D. S. & Sanson, B. Epithelial polarity and morphogenesis. *Curr. Opin. Cell Biol.* **23,** 540–546 (2011).
3. Thompson, B. J. Cell polarity: models and mechanisms from yeast, worms and flies. *Development* **140,** 13–21 (2012).
4. Ohno, S., Goulas, S. & Hirose, T. The PAR3-aPKC-PAR6 complex. in *Cell Polarity 1: Biological Role and Basic Mechanisms* 3–23 (2015). doi:10.1007/978-3-319-14463-4_1
5. Salinas-Saavedra, M., Stephenson, T. Q., Dunn, C. W. & Martindale, M. Q. Par system components are asymmetrically localized in ectodermal epithelia, but not during early development in the sea anemone Nematostella vectensis. *Evodevo* **6,** (2015).
6. Gumbiner, B. M. & Kim, N.-G. The Hippo-YAP signaling pathway and contact inhibition of growth. *J. Cell Sci.* **127,** 709–717 (2014).
7. Besson, C. *et al.* Planar Cell Polarity Breaks the Symmetry of PAR Protein Distribution prior to Mitosis in Drosophila Sensory Organ Precursor Cells. *Curr. Biol.* **25,** 1104–1110 (2015).
8. Yang, Y. & Mlodzik, M. Wnt-Frizzled/Planar Cell Polarity Signaling: Cellular Orientation by Facing the Wind (Wnt). *Annu. Rev. Cell Dev. Biol.* **31,** 623–646 (2015).
9. Ahmed, S. M. & Macara, I. G. Mechanisms of polarity protein expression control. *Curr. Opin. Cell Biol.* **42,** 38–45 (2016).
10. Aigouy, B. & Le Bivic, A. The PCP pathway regulates Baz planar distribution in epithelial cells. *Nat. Publ. Gr.* 1–11 (2016). doi:10.1038/srep33420
11. Butler, M. T. & Wallingford, J. B. Planar cell polarity in development and disease. *Nat. Rev. Mol. Cell Biol.* **18,** 375 (2017).
12. Davey, C. F. & Moens, C. B. Planar cell polarity in moving cells: think globally, act locally.

Development **144,** 187–200 (2017).

13. Fanto, M. Planar polarity from flies to vertebrates. *J. Cell Sci.* **117,** 527–533 (2004).
14. St Johnston, D. & Ahringer, J. Cell Polarity in Eggs and Epithelia: Parallels and Diversity. *Cell* **141,** 757–774 (2010).
15. Cha, S.-W., Tadjuidje, E., Wylie, C. & Heasman, J. The roles of maternal Vangl2 and aPKC in Xenopus oocyte and embryo patterning. *Development* **138,** 3989–4000 (2011).
16. Kumburegama, S., Wijesena, N., Xu, R. & Wikramanayake, A. H. Strabismus-mediated primary archenteron invagination is uncoupled from Wnt/β-catenin-dependent endoderm cell fate specification in Nematostella vectensis (Anthozoa, Cnidaria): Implications for the evolution of gastrulation. *Evodevo* **2,** 2 (2011).
17. Nance, J. & Zallen, J. A. Elaborating polarity: PAR proteins and the cytoskeleton. *Development* **138,** 799–809 (2011).
18. Momose, T., Kraus, Y. & Houliston, E. A conserved function for Strabismus in establishing planar cell polarity in the ciliated ectoderm during cnidarian larval development. *Development* **139,** 4374–4382 (2012).
19. Wallingford, J. B. Planar cell polarity and the developmental control of cell behavior in vertebrate embryos. *Annu. Rev. Cell Dev. Biol.* **28,** 627–653 (2012).
20. Fahey, B. & Degnan, B. M. Origin of animal epithelia: insights from the sponge genome. *Evol. & Dev.* **12,** 601–617 (2010).
21. Ragkousi, K., Marr, K., McKinney, S., Ellington, L. & Gibson, M. C. Cell-Cycle-Coupled Oscillations in Apical Polarity and Intercellular Contact Maintain Order in Embryonic Epithelia. *Curr. Biol.* 1–19 (2017). doi:10.1016/j.cub.2017.03.064
22. Salinas-Saavedra, M., Rock, A. Q. & Martindale, M. Q. Germ layer-specific regulation of cell polarity and adhesion gives insight into the evolution of mesoderm. *Elife* **7,** (2018).
23. Belahbib, H. *et al.* New genomic data and analyses challenge the traditional vision of animal

epithelium evolution. *BMC Genomics* **19,** 393 (2018).

24. Dunn, C. W. *et al.* Broad phylogenomic sampling improves resolution of the animal tree of life. *Nature* **452,** 745–749 (2008).
25. Hejnol, A. *et al.* Assessing the root of bilaterian animals with scalable phylogenomic methods. *Proc. Biol. Sci.* **276,** 4261–4270 (2009).
26. Ryan, J. F. *et al.* The Genome of the Ctenophore Mnemiopsis leidyi and Its Implications for Cell Type Evolution. *Science (80-.).* **342,** 1242592 (2013).
27. Moroz, L. L. *et al.* The ctenophore genome and the evolutionary origins of neural systems. *Nature* **510,** 109–114 (2014).
28. Whelan, N. V *et al.* Ctenophore relationships and their placement as the sister group to all other animals. *Nat. Ecol. & Evol.* 1–10 (2017). doi:10.1038/s41559-017-0331-3
29. Etienne-Manneville, S. Cdc42 - the centre of polarity. *J. Cell Sci.* **117,** 1291–1300 (2004).
30. Hutterer, A., Betschinger, J., Petronczki, M. & Knoblich, J. A. Sequential roles of Cdc42, Par-6, aPKC, and Lgl in the establishment of epithelial polarity during Drosophila embryogenesis. *Dev. Cell* **6,** 845–854 (2004).
31. Whitney, D. S. *et al.* Binding of Crumbs to the Par-6 CRIB-PDZ Module Is Regulated by Cdc42. *Biochemistry* **55,** 1455–1461 (2016).
32. Kim, S. H., Li, Z. & Sacks, D. B. E-cadherin-mediated Cell-Cell Attachment Activates Cdc42. *J Biol Chem* **275,** 36999–37005 (2000).
33. Schäfer, G., Narasimha, M., Vogelsang, E. & Leptin, M. Cadherin switching during the formation and differentiation of the Drosophila mesoderm - implications for epithelial-to-mesenchymal transitions. *J. Cell Sci.* **127,** 1511–1522 (2014).
34. Weng, M. & Wieschaus, E. Polarity protein Par3/Bazooka follows myosin-dependent junction repositioning. *Dev. Biol.* **422,** 125–134 (2017).
35. Harris, T. J. C. & Peifer, M. Adherens junction-dependent and -independent steps in the

establishment of epithelial cell polarity in Drosophila. *J. Cell Biol.* **167,** 135–147 (2004).

36. Nelson, W. J. & Nusse, R. Convergence of Wnt, β-Catenin, and Cadherin pathways. *Science (80-.).* **303,** 1483–1487 (2004).
37. McGill, M. A., McKinley, R. F. A. & Harris, T. J. C. Independent cadherin-catenin and Bazooka clusters interact to assemble adherens junctions. *J. Cell Biol.* **185,** 787–796 (2009).
38. Oda, H. & Takeichi, M. Structural and functional diversity of cadherin at the adherens junction. *J. Cell Biol.* **193,** 1137–1146 (2011).
39. Weng, M. & Wieschaus, E. Myosin-dependent remodeling of adherens junctions protects junctions from Snail-dependent disassembly. *J. Cell Biol.* **212,** 219–229 (2016).
40. Benton, R. & St Johnston, D. Drosophila PAR-1 and 14-3-3 inhibit Bazooka/PAR-3 to establish complementary cortical domains in polarized cells. *Cell* **115,** 691–704 (2003).
41. Hurov, J. B., Watkins, J. L. & Piwnica-Worms, H. Atypical PKC phosphorylates PAR-1 kinases to regulate localization and activity. *Curr. Biol.* **14,** 736–741 (2004).
42. Zhang, Y. *et al.* PAR-1 Kinase Phosphorylates Dlg and Regulates Its Postsynaptic Targeting at the Drosophila Neuromuscular Junction. *Neuron* **53,** 201–215 (2007).
43. Iden, S. & Collard, J. G. Crosstalk between small GTPases and polarity proteins in cell polarization. *Nat. Rev. Mol. cell Biol.* **9,** 846–859 (2008).
44. Yamanaka, T. & Ohno, S. Role of Lgl/Dlg/Scribble in the regulation of epithelial junction, polarity and growth. *Front Biosci* **13,** 6693–6707 (2008).
45. Oshima, K. & Fehon, R. G. Analysis of protein dynamics within the septate junction reveals a highly stable core protein complex that does not include the basolateral polarity protein Discs large. *J. Cell Sci.* **124,** 2861–2871 (2011).
46. Ganot, P. *et al.* Structural molecular components of septate junctions in cnidarians point to the origin of epithelial junctions in eukaryotes. *Mol. Biol. Evol.* **32,** 44–62 (2015).
47. Humbert, P. O., Russell, S. M., Smith, L. & Richardson, H. E. The scribble--Dlg--Lgl module

in cell polarity regulation. in *Cell Polarity 1* 65–111 (Springer, 2015).

48. Kharfallah, F. *et al.* Scribble1 plays an important role in the pathogenesis of neural tube defects through its mediating effect of Par-3 and Vangl1/2 localization. *Hum. Mol. Genet.* **26,** 2307–2320 (2017).

49. Lim, J. & Thiery, J. P. Epithelial-mesenchymal transitions: insights from development. *Development* **139,** 3471–3486 (2012).

50. Nieto, M. A., Huang, R. Y.-J., Jackson, R. A. & Thiery, J. P. EMT: 2016. *Cell* **166,** 21–45 (2016).

51. Ohsawa, S., Vaughen, J. & Igaki, T. Cell Extrusion: A Stress-Responsive Force for Good or Evil in Epithelial Homeostasis. *Dev. Cell* **44,** 284–296 (2018).

52. Ossipova, O., Dhawan, S., Sokol, S. & Green, J. B. A. Distinct PAR-1 proteins function in different branches of Wnt signaling during vertebrate development. *Dev. Cell* **8,** 829–841 (2005).

53. Munro, E. M. PAR proteins and the cytoskeleton: a marriage of equals. *Curr. Opin. Cell Biol.* **18,** 86–94 (2006).

54. Patalano, S. *et al.* The aPKC-PAR-6-PAR-3 cell polarity complex localizes to the centrosome attracting body, a macroscopic cortical structure responsible for asymmetric divisions in the early ascidian embryo. *J. Cell Sci.* **119,** 1592–1603 (2006).

55. Goldstein, B. & Macara, I. G. The PAR proteins: fundamental players in animal cell polarization. *Dev. Cell* **13,** 609–622 (2007).

56. Weisblat, D. A. Asymmetric cell divisions in the early embryo of the leech Helobdella robusta. *Prog. Mol. Subcell. Biol.* **45,** 79–95 (2007).

57. Alford, L. M., Ng, M. M. & Burgess, D. R. Cell polarity emerges at first cleavage in sea urchin embryos. *Dev. Biol.* **330,** 12–20 (2009).

58. Munro, E. & Bowerman, B. Cellular symmetry breaking during Caenorhabditis elegans

development. *Cold Spring Harb. Perspect. Biol.* **1,** (2009).

59. Doerflinger, H. *et al.* Bazooka is required for polarisation of the Drosophila anterior-posterior axis. *Development* **137,** 1765–1773 (2010).

60. Chan, E. & Nance, J. Mechanisms of CDC-42 activation during contact-induced cell polarization. *J. Cell Sci.* **126,** 1692–1702 (2013).

61. Lang, C. F. & Munro, E. The PAR proteins: from molecular circuits to dynamic self-stabilizing cell polarity. *Development* **144,** 3405–3416 (2017).

62. Tepass, U. The apical polarity protein network in Drosophila epithelial cells: regulation of polarity, junctions, morphogenesis, cell growth, and survival. *Annu. Rev. Cell Dev. Biol.* **28,** 655–685 (2012).

63. Zhu, M., Leung, C. Y., Shahbazi, M. N. & Zernicka-Goetz, M. Actomyosin polarisation through PLC-PKC triggers symmetry breaking of the mouse embryo. *Nat. Commun.* 1–16 (2017).

64. Schneider, S. Q. & Bowerman, B. Cell polarity and the cytoskeleton in the Caenorhabditis elegans zygote. *Annu. Rev. Genet.* **37,** 221–249 (2003).

65. Macara, I. G. Parsing the polarity code. *Nat. Rev. Mol. cell Biol.* **5,** 220–231 (2004).

66. Vinot, S., Le, T., Maro, B. & Louvet-Vallée, S. Two PAR6 proteins become asymmetrically localized during establishment of polarity in mouse oocytes. *Curr. Biol.* **14,** 520–525 (2004).

67. Dollar, G. L., Weber, U., Mlodzik, M. & Sokol, S. Y. Regulation of Lethal giant larvae by Dishevelled. *Nature* **437,** 1376–1380 (2005).

68. Kemphues, K. J., Priess, J. R., Morton, D. G. & Cheng, N. S. Identification of genes required for cytoplasmic localization in early C. elegans embryos. *Cell* **52,** 311–320 (1988).

69. Nance, J. Cell biology in development: Getting to know your neighbor: Cell polarization in early embryos. *J. Cell Biol.* **206,** 823–832 (2014).

70. Fritzenwanker, J. H., Genikhovich, G., Kraus, Y. & Technau, U. Early development and axis

specification in the sea anemone Nematostella vectensis. *Dev. Biol.* **310,** 264–279 (2007).

71. Lee, P. N., Kumburegama, S., Marlow, H. Q., Martindale, M. Q. & Wikramanayake, A. H. Asymmetric developmental potential along the animal-vegetal axis in the anthozoan cnidarian, Nematostella vectensis, is mediated by Dishevelled. *Dev. Biol.* **310,** 169–186 (2007).

72. Martindale, M. Q. & Henry, J. Q. Reassessing embryogenesis in the Ctenophora: the inductive role of e1 micromeres in organizing ctene row formation in the 'mosaic' embryo, Mnemiopsis leidyi. *Development* **124,** 1999–2006 (1997).

73. Martindale, M. Q. & Henry, J. Q. Intracellular fate mapping in a basal metazoan, the ctenophore Mnemiopsis leidyi, reveals the origins of mesoderm and the existence of indeterminate cell lineages. *Dev. Biol.* **214,** 243–257 (1999).

74. Pang, K. & Martindale, M. Q. Mnemiopsis leidyi spawning and embryo collection. *Cold Spring Harb. Protoc.* (2008). doi:10.1101/pdb.prot5085

75. Fischer, A. H. L., Pang, K., Henry, J. Q. & Martindale, M. Q. A cleavage clock regulates features of lineage-specific differentiation in the development of a basal branching metazoan, the ctenophore Mnemiopsis leidyi. *Evodevo* **5,** 0–19 (2014).

76. Nakaya, M. *et al.* Meiotic maturation induces animal-vegetal asymmetric distribution of aPKC and ASIP/PAR-3 in Xenopus oocytes. *Development* **127,** 5021–5031 (2000).

77. Etienne-Manneville, S. & Hall, A. Cell polarity: Par6, aPKC and cytoskeletal crosstalk. *Curr. Opin. Cell Biol.* **15,** 67–72 (2003).

78. Vinot, S. *et al.* Asymmetric distribution of PAR proteins in the mouse embryo begins at the 8-cell stage during compaction. *Dev. Biol.* **282,** 307–319 (2005).

79. Pruliere, G., Cosson, J., Chevalier, S., Sardet, C. & Chênevert, J. Atypical protein kinase C controls sea urchin ciliogenesis. *Mol. Biol. Cell* **22,** 2042–2053 (2011).

80. Lu, M. S. & Johnston, C. A. Molecular pathways regulating mitotic spindle orientation in

animal cells. *Development* **140,** 1843–1856 (2013).

81. Hoege, C. & Hyman, A. A. Principles of PAR polarity in Caenorhabditis elegans embryos. *Nat. Rev. Mol. cell Biol.* **14,** 315–322 (2013).

82. Von Stetina, S. E. & Mango, S. E. PAR-6, but not E-cadherin and β-integrin, is necessary for epithelial polarization in C. elegans. *Dev. Biol.* **403,** 5–14 (2015).

83. Martindale, M. Q. The ontogeny and maintenance of adult symmetry properties in the ctenophore, Mnemiopsis mccradyi. *Dev. Biol.* **118,** 556–576 (1986).

84. Henry, J. Q. & Martindale, M. Q. Regulation and regeneration in the ctenophore Mnemiopsis leidyi. *Dev. Biol.* **227,** 720–733 (2000).

85. Henry, J. Q. & Martindale, M. Q. Inductive interactions and embryonic equivalence groups in a basal metazoan, the ctenophore Mnemiopsis leidyi. *Evol. & Dev.* **6,** 17–24 (2004).

86. Campanale, J. P., Sun, T. Y. & Montell, D. J. Development and dynamics of cell polarity at a glance. *J. Cell Sci.* **130,** 1201–1207 (2017).

87. Knust, E. & Bossinger, O. Composition and formation of intercellular junctions in epithelial cells. *Science (80-.).* **298,** 1955–1959 (2002).

88. Tyler, S. Epithelium—the primary building block for metazoan complexity. *Integr. Comp. Biol.* **43,** 55–63 (2003).

89. Woods, D. F., Wu, J. W. & Bryant, P. J. Localization of proteins to the apico-lateral junctions of Drosophila epithelia. *Dev. Genet.* **20,** 111–118 (1997).

90. Bilder, D., Li, M. & Perrimon, N. Cooperative regulation of cell polarity and growth by Drosophila tumor suppressors. *Science (80-.).* **289,** 113–116 (2000).

91. Vaccari, T., Rabouille, C. & Ephrussi, A. The Drosophila PAR-1 spacer domain is required for lateral membrane association and for polarization of follicular epithelial cells. *Curr. Biol.* **15,** 255–261 (2005).

92. Cox, D. N., Lu, B., Sun, T.-Q., Williams, L. T. & Jan, Y. N. Drosophila par-1 is required for

oocyte differentiation and microtubule organization. *Curr. Biol.* **11,** 75–87 (2001).

93. Tian, A.-G. & Deng, W.-M. Par-1 and Tau regulate the anterior-posterior gradient of microtubules in Drosophila oocytes. *Dev. Biol.* **327,** 458–464 (2009).

94. Motegi, F. *et al.* Microtubules induce self-organization of polarized PAR domains in Caenorhabditis elegans zygotes. *Nat. Cell Biol.* **13,** 1361–1367 (2011).

95. Timm, T. *et al.* Microtubule affinity regulating kinase activity in living neurons was examined by a genetically encoded fluorescence resonance energy transfer/fluorescence lifetime imaging-based biosensor: inhibitors with therapeutic potential. *J Biol Chem* **286,** 41711–41722 (2011).

96. Chalmers, A. D. *et al.* aPKC, Crumbs3 and Lgl2 control apicobasal polarity in early vertebrate development. *Development* **132,** 977–986 (2005).

97. Hayase, J. *et al.* The WD40 protein Morg1 facilitates Par6-aPKC binding to Crb3 for apical identity in epithelial cells. *J. Cell Biol.* **200,** 635–650 (2013).

98. Wikramanayake, A. H. *et al.* An ancient role for nuclear catenin in the evolution of axial polarity and germ layer segregation. *Nature* **426,** 446–450 (2003).

99. Martindale, M. Q. & Hejnol, A. A developmental perspective: changes in the position of the blastopore during bilaterian evolution. *Dev. Cell* **17,** 162–174 (2009).

100. Martindale, M. Q. & Lee, P. N. The Development of Form: Causes and Consequences of Developmental Reprogramming Associated with Rapid Body Plan Evolution in the Bilaterian Radiation. *Biol. Theory* **8,** 253–264 (2013).

101. Pang, K. *et al.* Genomic insights into Wnt signaling in an early diverging metazoan, the ctenophore Mnemiopsis leidyi. *Evodevo* **1,** 10 (2010).

102. Humbert, P. O., Dow, L. E. & Russell, S. M. The Scribble and Par complexes in polarity and migration: friends or foes? *Trends in Cell Biology* **16,** 622–630 (2006).

103. Seifert, J. R. K. & Mlodzik, M. Frizzled/PCP signaling: a conserved mechanism regulating cell

polarity and directed motility. *Nat Rev Genet* **8,** 126–138 (2007).

104. Newman, S. A. & Bhat, R. Dynamical patterning modules: a "pattern language" for development and evolution of multicellular form. *Int. J. Dev. Biol.* **53,** 693–705 (2009).

105. Newman, S. A. Animal egg as evolutionary innovation: a solution to the "embryonic hourglass" puzzle. *J. Exp. Zool. Part B Mol. Dev. Evol.* (2011). doi:10.1002/jez.b.21417

106. Babonis, L. S. & Martindale, M. Q. Phylogenetic evidence for the modular evolution of metazoan signalling pathways. *Philos. Trans. R. Soc. B Biol. Sci.* **372,** 20150419–20150477 (2017).

107. Salinas-Saavedra, M. & Martindale, M. Q. Improved protocol for spawning and immunostaining embryos and juvenile stages of the ctenophore Mnemiopsis leidyi. *Protoc. Exch.* (2018). doi:10.1038/protex.2018.092

108. Roure, A. *et al.* A multicassette Gateway vector set for high throughput and comparative analyses in ciona and vertebrate embryos. *PLoS One* **2,** e916 (2007).

109. DuBuc, T. Q. *et al.* In vivo imaging of Nematostella vectensis embryogenesis and late development using fluorescent probes. *BMC Cell Biol.* **15,** 44 (2014).

110. Layden, M. J., Röttinger, E., Wolenski, F. S., Gilmore, T. D. & Martindale, M. Q. Microinjection of mRNA or morpholinos for reverse genetic analysis in the starlet sea anemone, Nematostella vectensis. *Nat. Protoc.* **8,** 924–934 (2013).

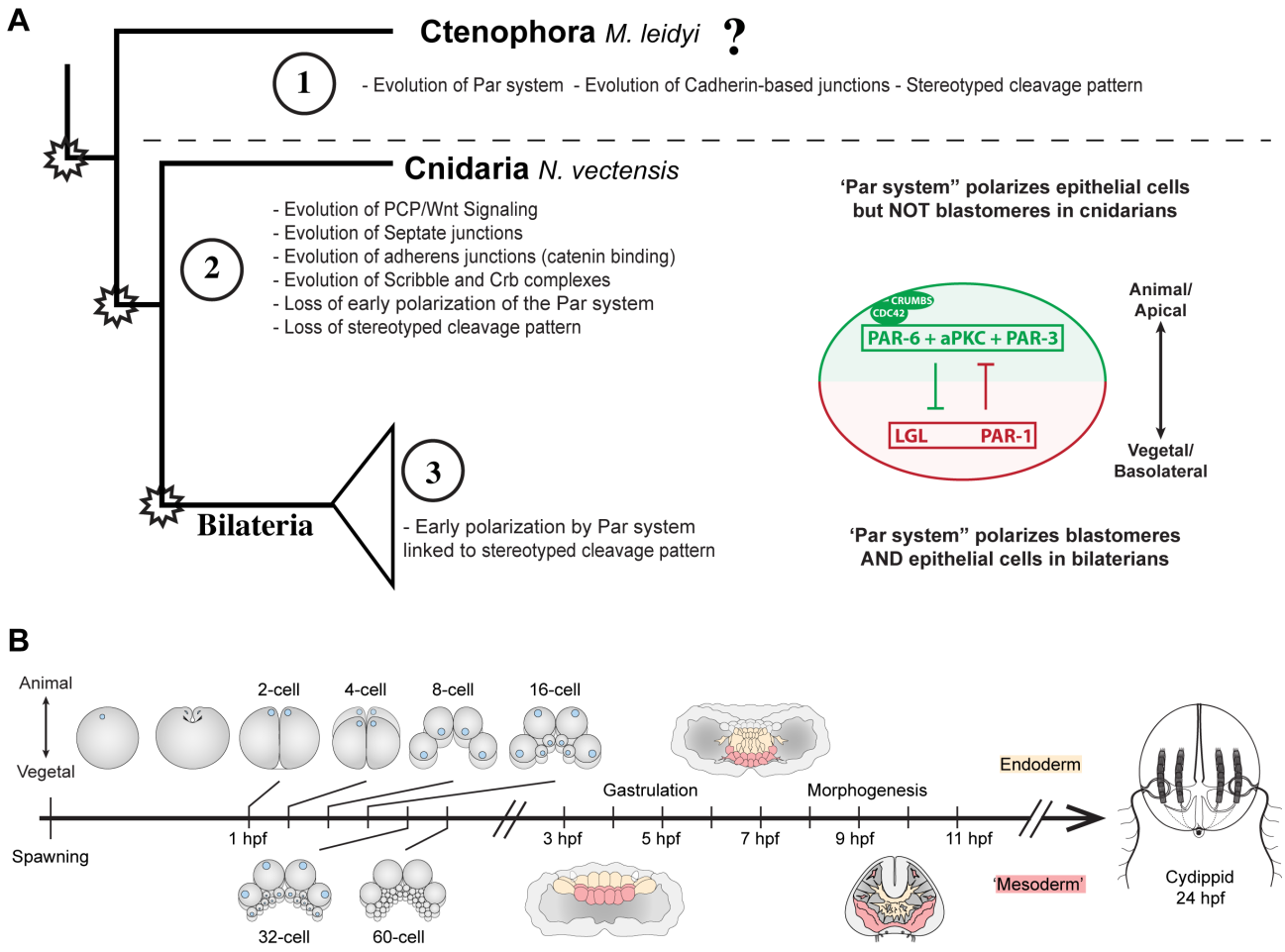

Figure 1. Evolution of cell polarity components during the animal evolution. A) Three major evolutionary steps (left side) that might have changed the organization of cell polarity in the Metazoa. The diagram (right side) depicts the subcellular asymmetric localization of Par proteins in Cnidaria and Bilateria. However, there are no descriptions available for ctenophore cells B) The stereotyped early development of *M. leidyi*.

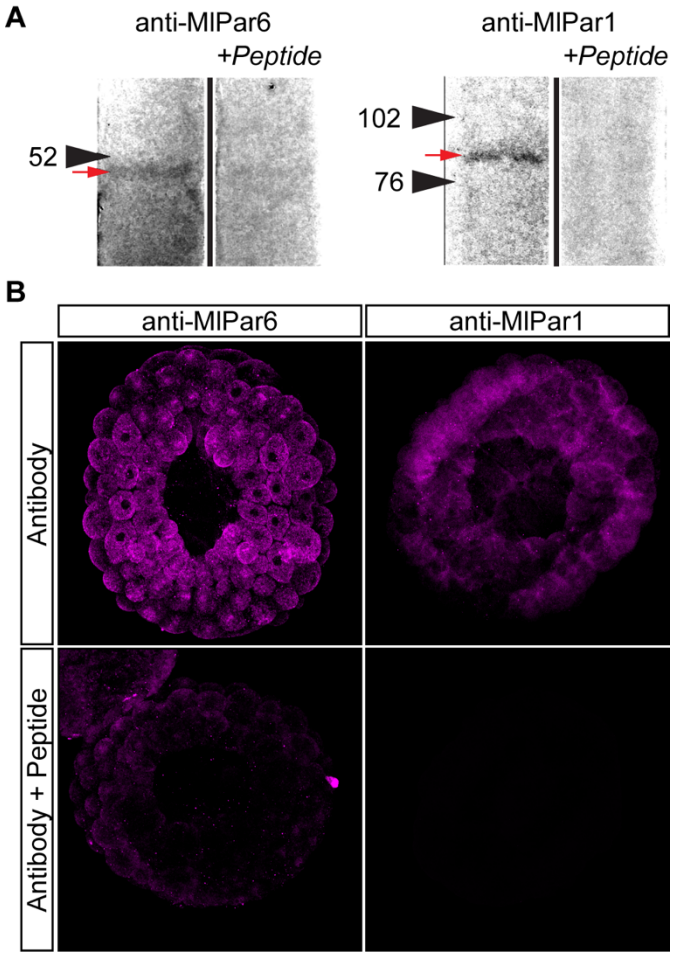

Figure 2. Specificity of *M. leidyi* antibodies tested by pre-adsorption experiments. A) Western blots of *M. leidyi* adult tissue extracts using specific antibodies against *Ml*Par-6 and *Ml*Par-1. Pre-adsorption of the antibodies with a tenfold excess of the antigen peptide resulted in the titration of *Ml*Par-6 and the elimination of the staining of a single band for *Ml*Par-1. Arrowheads indicate the molecular weight in KD. A red arrow indicates the band recognized by the antibody for each protein. B) Whole-mount immunohistochemistry pre-adsorption experiments show that the staining pattern was strongly mitigated in early embryos when pre-incubated antibodies against *Ml*Par-6 and *Ml*Par-1 with the respective peptide.

Figure 3. *Ml*Par-6 protein localizes asymmetrically in the cell cortex of the eggs and in the cell-contact-free regions of cleavage stages. A) Immunostaining against *Ml*Par-6 during cleavage stages of *M. leidyi* development. *Ml*Par-6 protein localizes to the apical cortex (white arrows) until 60-cell stage where its signal was detected in cell-contact regions (white arrowhead). Images are 3D reconstructions from a z-stack confocal series. B) A single optical section from the 8-cell stage z-stack confocal series shown in A. *Ml*Par-6 protein localizes to the apical cortex of the cells but is absent from cell-contact regions. Orientation axes are depicted in the figure. C) Diagram depicting the cortical localization of *Ml*Par-6. Animal pole is to the top as depicted in B. Morphology is shown by DAPI and Tubulin immunostainings. Yellow arrowhead indicates the zygote nucleus. Yellow arrows indicate nuclear localization. Homogeneous cytosolic staining was digitally reduced to highlight cortical localizations.

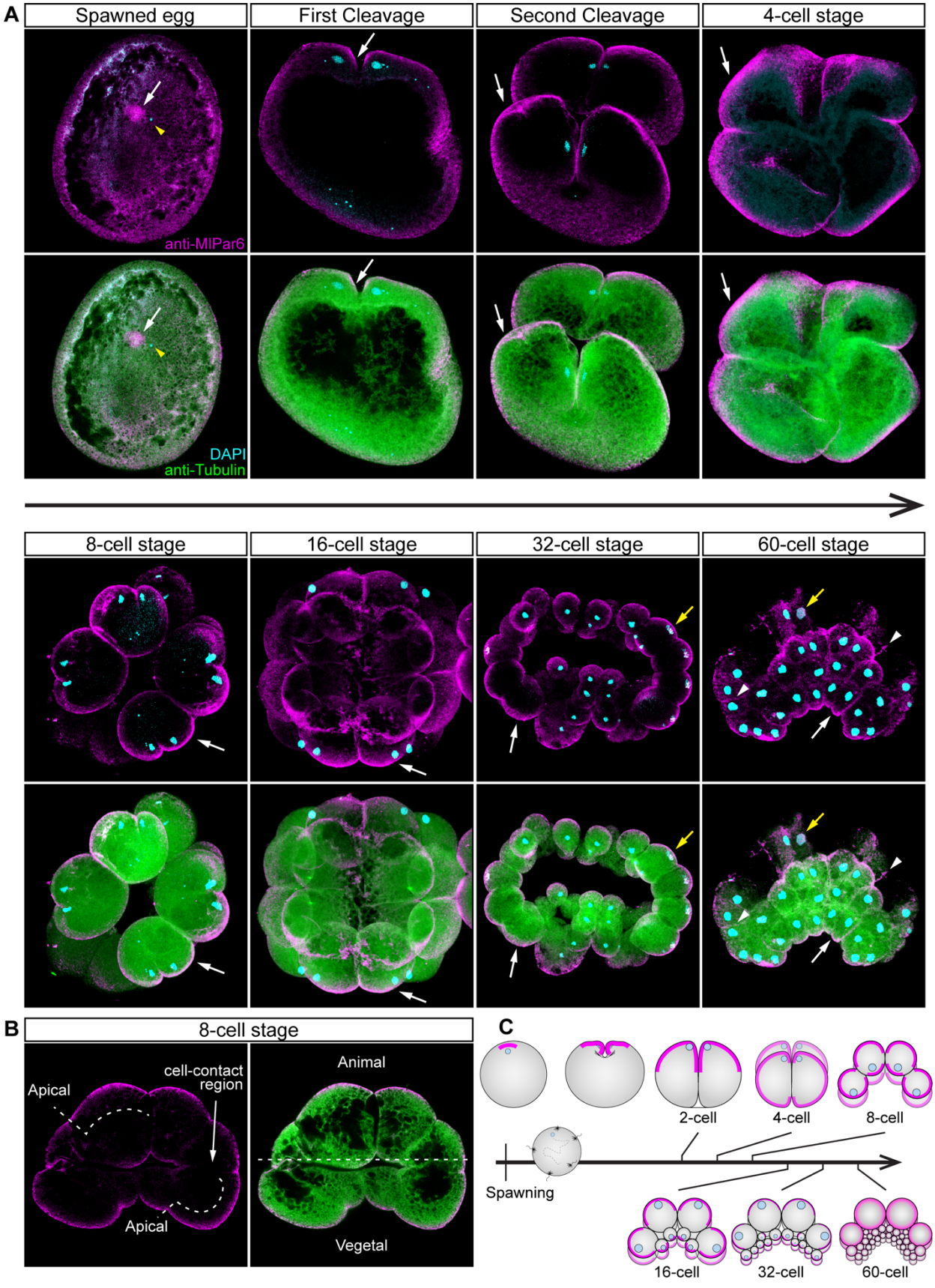

Figure 4. *Ml*Par-6 protein remains apically polarized in 'static' ectodermal cells during *M. leidyi* gastrulation. A) Immunostaining against *Ml*Par-6 during gastrulation stages of *M. leidyi* development. *Ml*Par-6 protein localizes to the apical cortex (white arrows) but it is not localized in cells undergoing cellular movements. Images are 3D reconstructions from a z-stack confocal series. B) A single optical section from the 6 hpf embryo z-stack confocal series shown in A. *Ml*Par-6 protein localizes to the apical cortex of the ectodermal cells (Ecto) but is absent from endodermal (Endo) and 'mesodermal' ('Meso') cells. Orientation axes are depicted in the figure. C) Diagram depicting the cortical localization of *Ml*Par-6 (Magenta). Endoderm and 'mesoderm' are colored in yellow and red, respectively. Blue arrows depict gastrulation movements. Animal pole is to the top as depicted in B. Morphology is shown by DAPI and Tubulin immunostainings. white arrowheads indicate *Ml*Par-6 protein in cell-contact regions. Yellow arrowheads indicate the absence of cortical localization. Homogeneous cytosolic staining was digitally reduced to highlight cortical localizations.

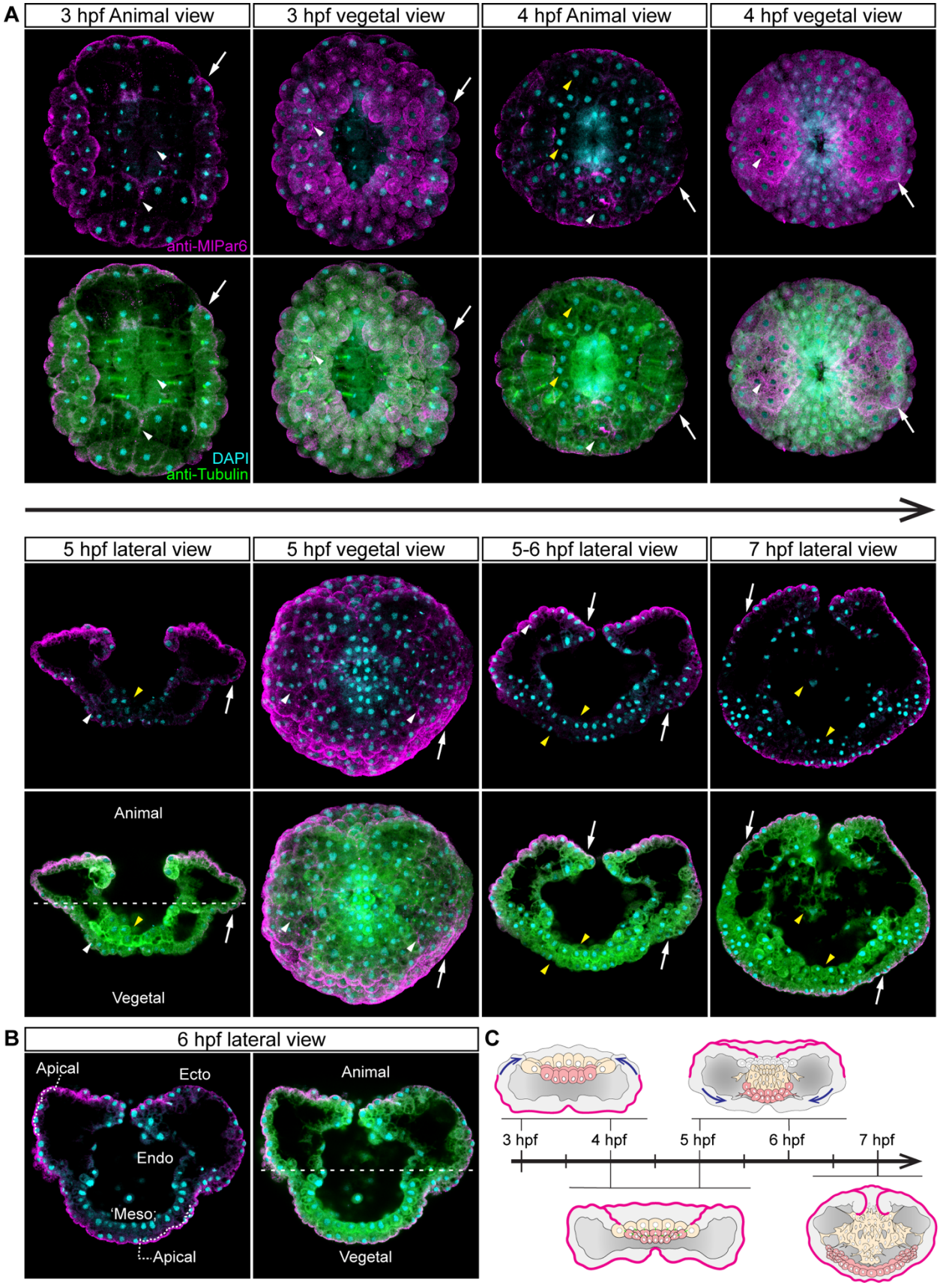

Figure 5. *Ml*Par-6 protein does not localize in the cortex of epidermal cells after 10 hpf during *M. leidyi* development. A) Immunostaining against *Ml*Par-6 during gastrulation stages of *M. leidyi* development. *Ml*Par-6 protein localizes to the apical cortex (white arrows) until 9 hpf but it is not cortically localized after 10 hpf. All 8-9 hpf images are single optical sections from a z-stack confocal series. 10-11 hpf images are 3D reconstructions from a z-stack confocal series. Orientation axes are depicted in the figure: Animal/oral pole is to the top. Morphology is shown by DAPI and Tubulin immunostainings. White arrowhead indicates *Ml*Par-6 protein in pharyngeal cells. Yellow arrowheads indicate nuclear localizations. B) *In vivo* localization of *Ml*Par6-mVenus during different stages of *M. leidyi* development. The overexpression of *Ml*Par6-mVenus protein displays similar patterns observed with the antibody staining against the same protein, and no cortical localization was observed after 10 hpf. All images are 3D reconstructions from a z-stack confocal series. Orientation axes are depicted in the figure: Animal/Oral pole is to the top. Morphology is shown by DIC microscopy. White arrows indicate *Ml*Par6-mVenus protein cortical localization. White arrowhead indicates *Ml*Par6-mVenus protein aggregates during early gastrulation movements. Yellow arrowheads indicate the absence of cortical localization and cytosolic aggregation. Homogeneous cytosolic staining was digitally reduced to highlight cortical localizations.

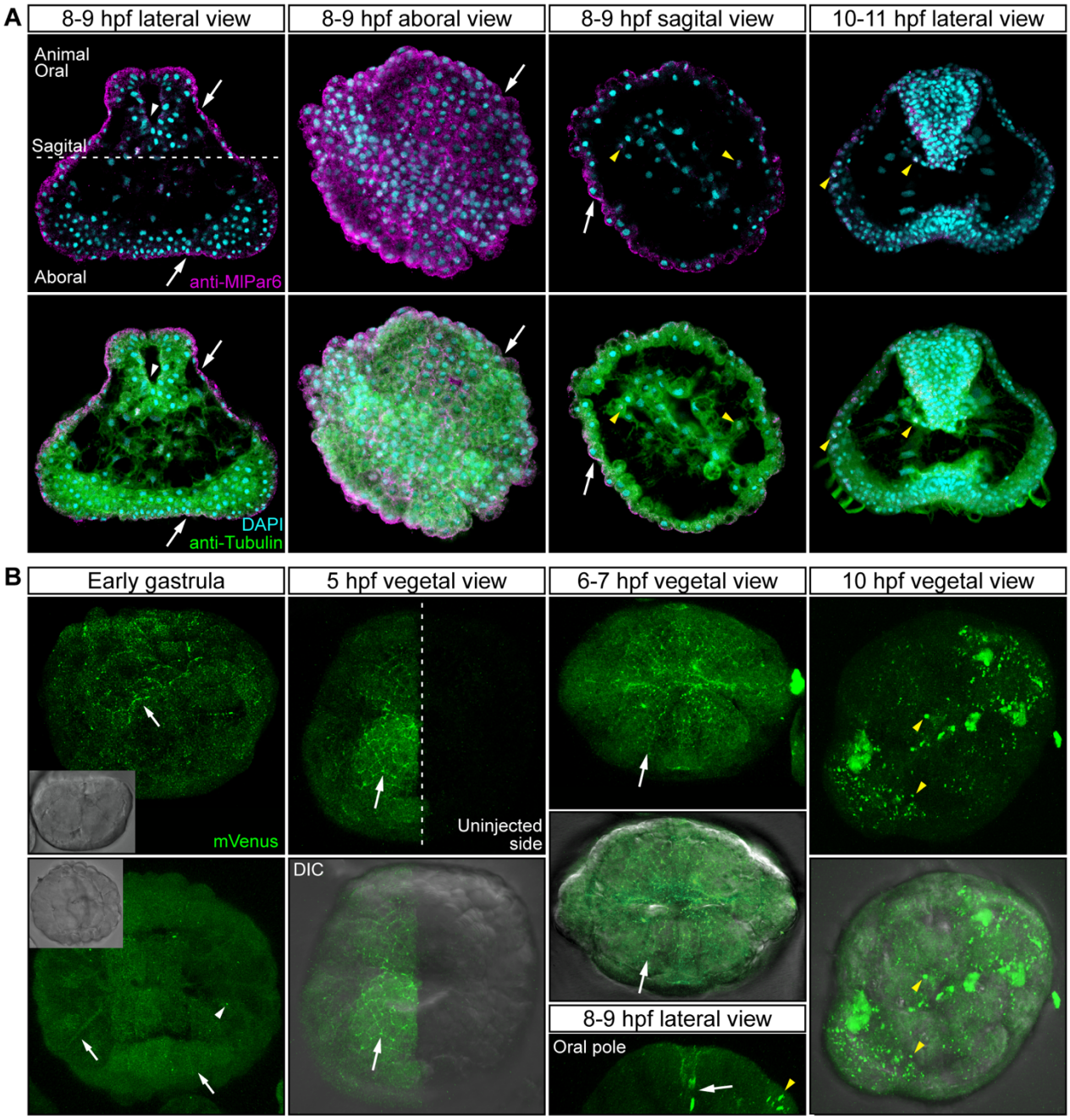

Figure 6. *Ml*Par-1 protein remains cytoplasmic during early cleavage stages. A) Immunostaining against *Ml*Par-1 during cleavage stages of *M. leidyi* development. *Ml*Par-1 protein remains as punctate aggregations distributed uniformly in the cytosol (white arrows). Images are 3D reconstructions from a z-stack confocal series. B) A single optical section from the 8-cell stage z-stack confocal series shown in A. *Ml*Par-1 appears to be localized in the cortex at the cell-contact regions but this antibody signal was not clear enough to be discriminated from its cytosolic distribution. C) Diagram depicting the localization of *Ml*Par-1. Animal pole is to the top. Morphology is shown by DAPI and Tubulin immunostainings. Yellow arrowhead indicates the zygote nucleus.

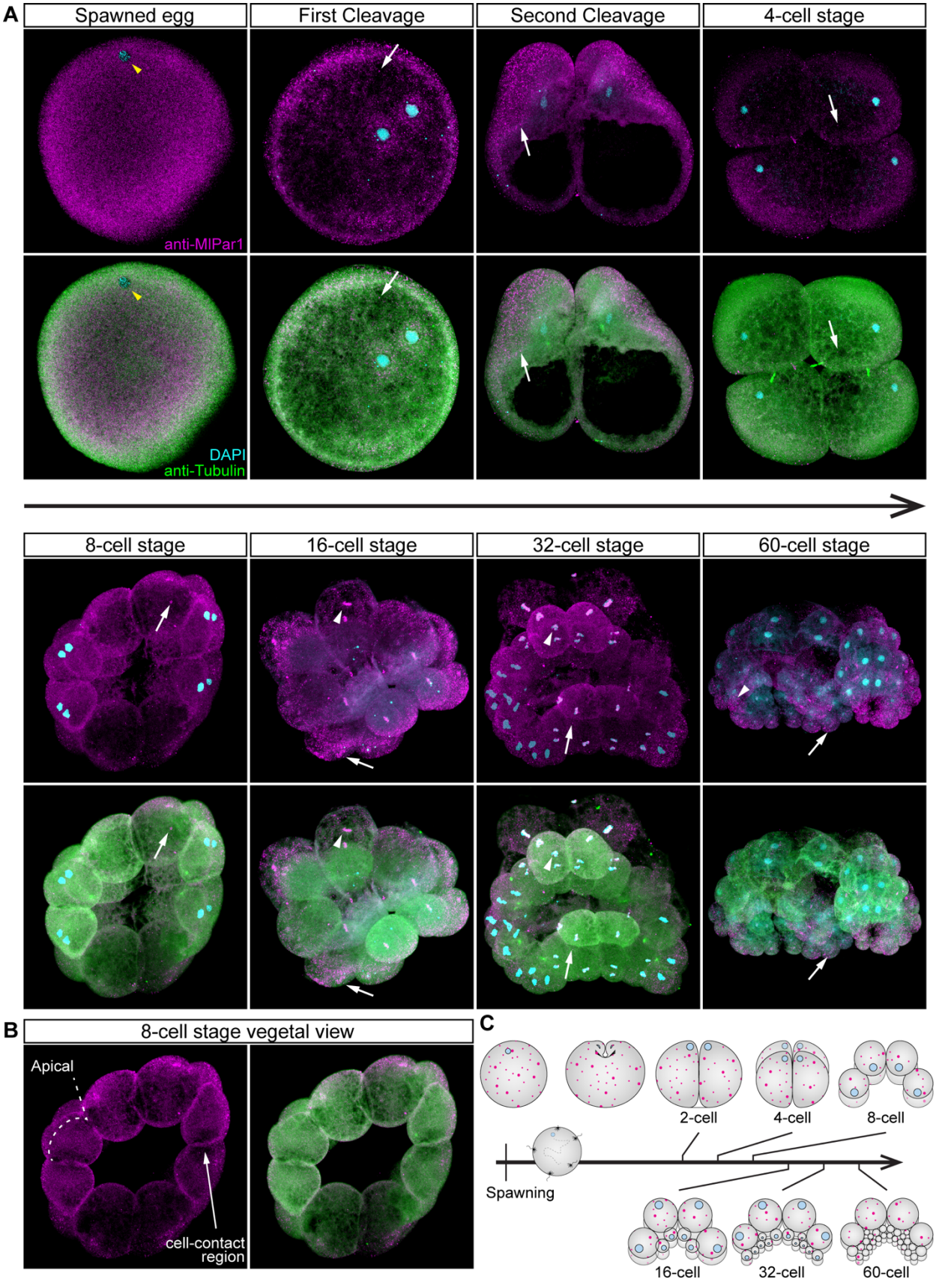

Figure 7. *Ml*Par-1 protein remains cytoplasmic during *M. leidyi* development. A) Immunostaining against *Ml*Par-1 after 3 hpf. *Ml*Par-1 protein remains as punctate aggregations distributed uniformly in the cytosol (white arrows). *Ml*Par-1 appears to be localized in the cortex at the cell-contact regions (white arrowheads) but this antibody signal was not clear enough to be discriminated from its cytosolic distribution. Images are 3D reconstructions from a z-stack confocal series. Orientation axes are depicted in the figure. B) A single optical section from the 8-9 hpf embryo z-stack confocal series shown in A. *Ml*Par-1 protein remains cytoplasmic in ectodermal cells (Ecto), endodermal (Endo), and 'mesodermal' ('Meso') cells. C) Diagram depicting the localization of *Ml*Par-1 (Magenta). Endoderm and 'mesoderm' are colored in yellow and red, respectively. Morphology is shown by DAPI and Tubulin immunostainings. Yellow arrowheads indicate nuclear localization. Animal pole is to the top.

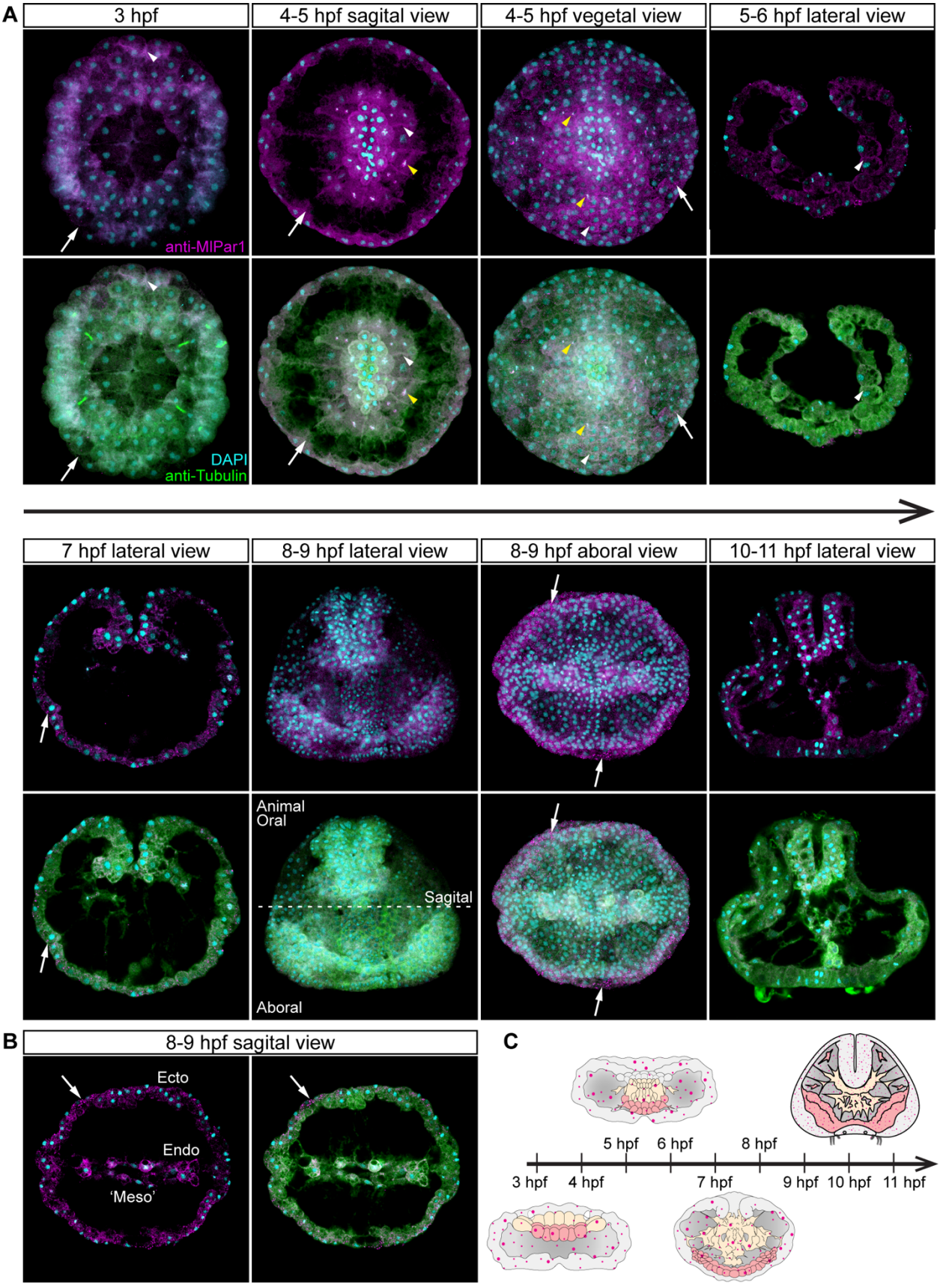

Figure 8. *In vivo* localization of *Ml*Par proteins during different stages of *M. leidyi* development. A) The overexpression of *Ml*Par1-mCherry protein displays similar patterns observed with the antibody staining against the same protein, and no cortical localization was observed after 4 hpf. White arrows indicate *Ml*Par-1-mCherry protein cytosolic aggregates. White arrowhead indicates *Ml*Par-1-mCherry protein aggregates in the tentacle apparatus. All images are 3D reconstructions from a z-stack confocal series. Orientation axes are depicted in the figure. B) When *Ml*Par6-mVenus and *Ml*Par1-mCherry are overexpressed each ctenophore mRNA into embryos of the cnidarian *N. vectensis*, the translated proteins display the same pattern than the previously described endogenous *N. vectensis* proteins (Salinas-Saavedra et al., 2015). White arrowheads indicate *Ml*Par6-mVenus and *Ml*Par1-mCherry cortical localization. All images are a single slide from a z-stack confocal series. C) *In vivo* localization of *Ml*Cdc42-mCherry. White arrows indicate *Ml*Cdc42-mCherry protein aggregates. All images are 3D reconstructions from a z-stack confocal series. D) *In vivo* localization of *Ml*aPKC-mVenus. White arrows indicate *Ml*aPKC-mVenus protein aggregates. All images are 3D reconstructions from a z-stack confocal series. Morphology is shown by DIC microscopy. Homogeneous cytosolic staining was digitally reduced to highlight cortical localizations.

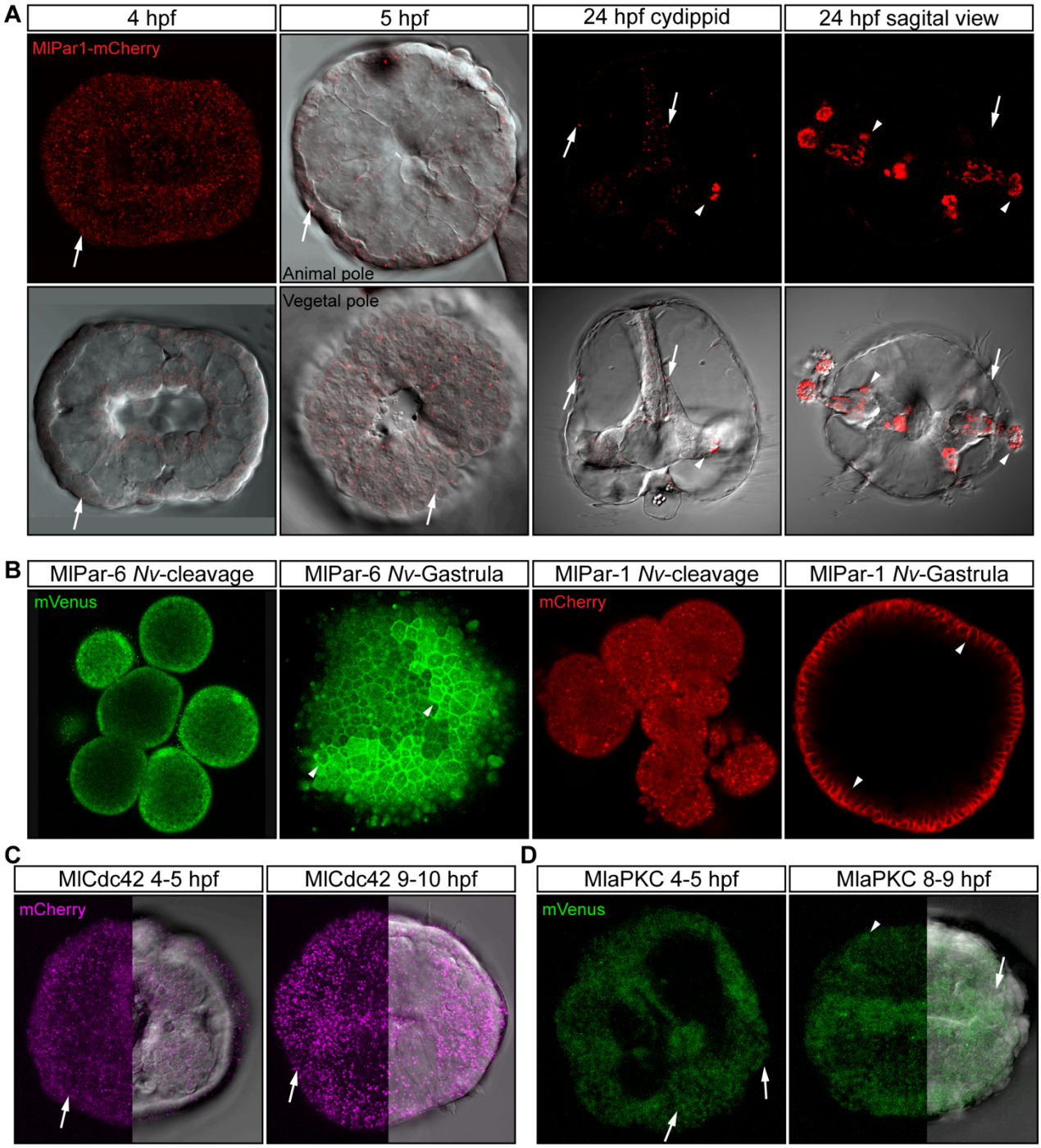

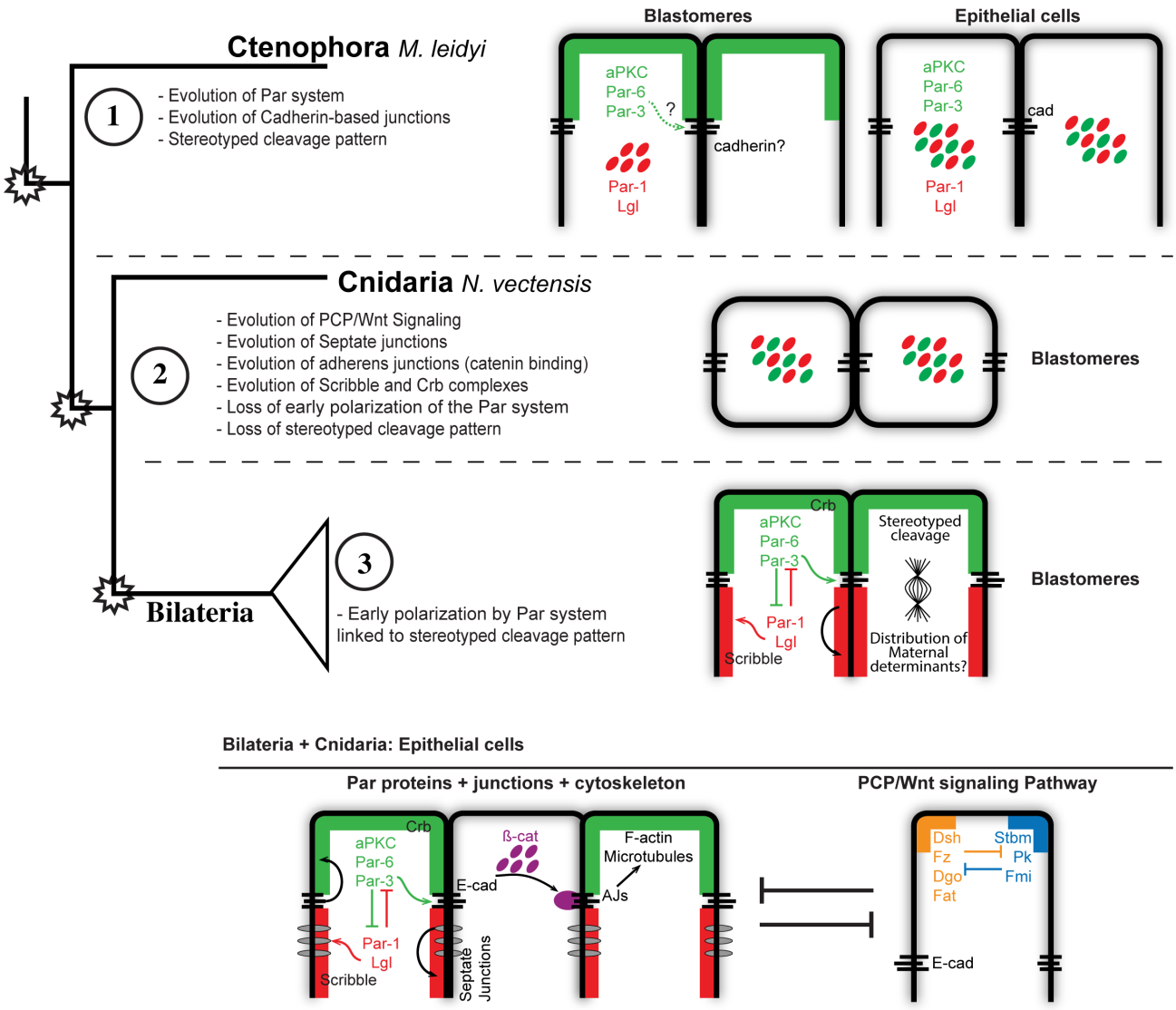

Figure 9. Evolution of cell polarity in Metazoa. Diagram depicting the evolution of different interactions between known signaling pathways that organize cell polarity in the Metazoa, including the new information obtained by this study during the early development of the ctenophore *M. leidyi*. Our results challenge the conception of a deep homology of the epithelial structure and the establishment of the apicobasal cell polarity in Metazoa.

Movie 1. Punctuate aggregates of *Ml*Par-1-mCherry are highly dynamics.

Key resources table

Reagent type (species) or resource	Designation	Source or reference	Identifiers	Additional information
Antibody	Mouse Anti-alpha-Tubulin Monoclonal Antibody, Unconjugated, Clone DM1A	Sigma-Aldrich	T9026; RRID:AB_477593	(1:500)
Antibody	anti-MlPar-6 custom peptide antibody produced in rabbit	Bethyl labs; This study		Stored at MQ Martindale's lab; (1:100)
Antibody	anti-MlPar-1 custom peptide antibody produced in rabbit	Bethyl labs; This study		Stored at MQ Martindale's lab; (1:100)
Antibody	Goat anti-Mouse IgG Secondary Antibody, Alexa Fluor 568	Thermo Fisher Scientific	A-11004; RRID:AB_2534072	(1:250)
Antibody	Goat anti-Rabbit IgG Secondary Antibody, Alexa Fluor 647	Thermo Fisher Scientific	A-21245; RRID:AB_2535813	(1:250)
Other	DAPI (4',6-Diamidino-2-Phenylindole, Dihydrochloride)	Thermo Fisher Scientific	D1306; RRID:AB_2629482	(0.1µg/µl)
Chemical compound, drug	Dextran, Alexa Fluor™ 488; 10,000 MW, Anionic, Fixable	Thermo Fisher Scientific	D22910	
Chemical compound, drug	Dextran, Alexa Fluor™ 555; 10,000 MW, Anionic, Fixable	Thermo Fisher Scientific	D34679	
Chemical compound, drug	Dextran, Alexa Fluor™ 647; 10,000 MW, Anionic, Fixable	Thermo Fisher Scientific	D22914	
Chemical compound, drug	Dextran, Cascade Blue™, 10,000 MW, Anionic, Lysine Fixable	Thermo Fisher Scientific	D1976	
Deposited Data	*Mnemiopsis Genome* Project	NIH-NHGRI	https://kona.nhgri.nih.gov/mnemiopsis/	
Sequence-based reagent	*Mlpar-6*: F-GTACTGTGCTGTGTGTTTGGA; R- GTACTGTGCTGTGTGTTTGGA		MLRB351777	
Sequence-based reagent	*Mlpar-1*: F- ATGTCAAATTCTCAACACCAC; R- CAGTCTTAATTCATTAGCTATGTTA		MLRB182569	
Sequence-based reagent	*MlCdc42*: F-TAGGAGTGTGCAGGGCTTTTT; R-TAGGAGTGTGCAGGGCTTTTT		ML049025a	
Sequence-based reagent	*MlaPKC*: F-ATGGATAGTTTGAATAGCAATAGTATAC; R- GACAGCTTCCTCCTTGTTGA		ML008317a	
Recombinant DNA reagent	pSPE3-mVenus	Roure et al., 2007		Gateway vector
Recombinant DNA reagent	pSPE3-mCherry	Roure et al., 2007		Gateway vector
Software, algorithm	Fiji (ImageJ)	NIH	http://fiji.sc	
Software, algorithm	Imaris 7.6.4	Bitplane Inc.		